Acta Ophthalmologica

Structural changes in the corneal subbasal nerve plexus in keratoconus

Elias Flockerzi, Loay Daas and Berthold Seitz

Department of Ophthalmology, Saarland University Medical Center, Homburg, Germany

ABSTRACT.

Background: **Corneal confocal microscopy (CCM) allows visualizing slightest alterations within the corneal subbasal nerve plexus (SNP). Recent CCM studies based on the analysis of three–five CCM images per eye assumed a reduced corneal nerve fibre length (CNFL) in keratoconus (KC).**

Methods: **The SNP of KC patients (n = 23, 13 contact lens wearing, 10 noncontact lens wearing) and patients without KC (n = 16) was examined by 10 CCM images of one eye per patient. The CNFL per frame area was calculated, and the SNP tortuosity was quantified by measuring (a) the amplitude of the curves and (b) the area under the curve (AUC) formed by the SNP.**

Results: **Analysing 390 non-overlapping confocal images revealed the CNFL (mm/mm^2) to be significantly lower in KC (16.4 ± 1.9 mm/mm^2) than in healthy corneae (23.8 ± 3.3 mm/mm^2, p < 0.0001; mean ± SD; p-value calculated using the Mann–Whitney *U*-test), without a difference between contact lens wearing and noncontact lens wearing KC patients (p = 0.4). Amplitudes and AUCs analysed as median with 25th and 75th percentile were significantly increased in KC (amplitude 33/23/41 μm and AUC 2839/1545/3444 μm^2) compared to healthy corneae (amplitude 24/18/28 μm and AUC 1870/1193/2327 μm^2, p < 0.0001).**

Conclusions: **Corneal confocal microscopy (CCM) visualizes slightest alterations within the SNP in KC including (a) a significantly lower CNFL and (b) an enhanced winding course of the SNP. The significantly lower CNFL observed in KC may support the hypothesis of a neurodegenerative aspect of the disease and might be a measure to be correlated with the severity and progression of the disease.**

Key words: corneal confocal microscopy – corneal nerve fibre length – keratoconus – subbasal nerve plexus

Acta Ophthalmol.

© 2020 The Authors. Acta Ophthalmologica Published by John Wiley & Sons Ltd on behalf of Acta Ophthalmologica Scandinavica Foundation

This is an open access article under the terms of the Creative Commons Attribution-NonCommercial License, which permits use, distribution and reproduction in any medium, provided the original work is properly cited and is not used for commercial purposes.

doi: 10.1111/aos.14432

Introduction

Keratoconus (KC) is an usually bilateral corneal ectasia of unknown aetiology with progressive and presumed non-inflammatory thinning of the cornea resulting in irregular astigmatism and visual impairment (Goebels et al. 2015). Therapy depends on progression of the disease and includes contact lens fitting, surgical treatment via cross-linking, implantation of corneal ring segments, deep anterior lamellar keratoplasty or penetrating keratoplasty (Goebels, Seitz & Langenbucher 2013). Clinical signs of KC do vary and depend on the stage of the disease. Corneal confocal microscopy (CCM) allows visualizing slightest alterations within the corneal subbasal nerve plexus (SNP) (Richter et al. 1997), which is formed by branches of the trigeminal nerve (Müller et al. 1997). Corneal confocal microscopy (CCM) studies based on the analysis of three (Simo Mannion, Tromans & O'Donnell 2005; Niederer et al. 2008; Song et al. 2016) to five (Bitirgen et al. 2013; Bitirgen et al. 2015; Köhler et al. 2017) corneal confocal images per eye, and patient indicated that there is a reduced corneal nerve fibre length (CNFL) and an abnormal winding course of the SNP in KC. But Allgeier et al. (2017) pointed out that reliable and reproducible data should be based on the analysis of at least 9.4 corneal confocal images corresponding to a minimum sampled area of 1.5 mm^2 of the central SNP. Several parameters have been proposed and were used to describe the abnormal structure of the SNP in KC including the corneal nerve fibre density, the corneal nerve branch density, the corneal total branch density, the corneal nerve fibre width and the corneal nerve fibre area (Petropoulos et al. 2014; Bitirgen et al. 2015; Pahuja et al. 2016). This study examined the SNP structure by analysis of 10 CCM images per eye in KC patients and healthy individuals and also proposes a novel way of quantifying the tortuous SNP course in KC visualized by CCM.

Patients and Methods

In this cross-sectional study, the SNP was examined in the central cornea of patients with KC (n = 23, 13 contact lens wearing, 10 noncontact lens

wearing) recruited from the Homburg Keratoconus Center (Goebels, Seitz & Langenbucher 2013) without history of hydrops corneae or ocular surgery, and of healthy, age-matched patients without KC or history of ocular surgery ($n = 16$). Several CCM images (400 μm × 400 μm, Figs 1 and 2) of one eye per patient were obtained by CCM using the Heidelberg Retina Tomograph (HRT, Heidelberg Engineering GmbH, Heidelberg, Germany) with the Rostock Cornea Module. Thereafter, overlapping images or images affected by motion artefacts were excluded after independent reviews by two authors (EF, LD). The investigators were masked to the KC stage in the KC group during the examination and masked to the patient groups during the CCM image selection. Finally, ten CCM images of one eye per patient or control were included for further analysis. Before examination, the patients' eyes were topically anaesthetized with proparacaine (proxymetacaine) 0.5% (Proparakain-POS® 0.5% eyedrops; Ursapharm, Saarbrücken, Germany); a carbomer (polyacrylic acid)-based formulation (Visc-Ophtal Sine®, Dr. Winzer Pharma, Berlin, Germany) was used as an epithelium-protective and coupling agent between the tomograph and the cornea. The patients were instructed to fixate on a distance target during the examination with the intention to reduce motion artefacts and to facilitate examination of the central cornea. It was aimed to exclude CCM images of the whorl and the corneal apex area in both healthy and KC corneae because of the more tortuous course of the SNP in this region.

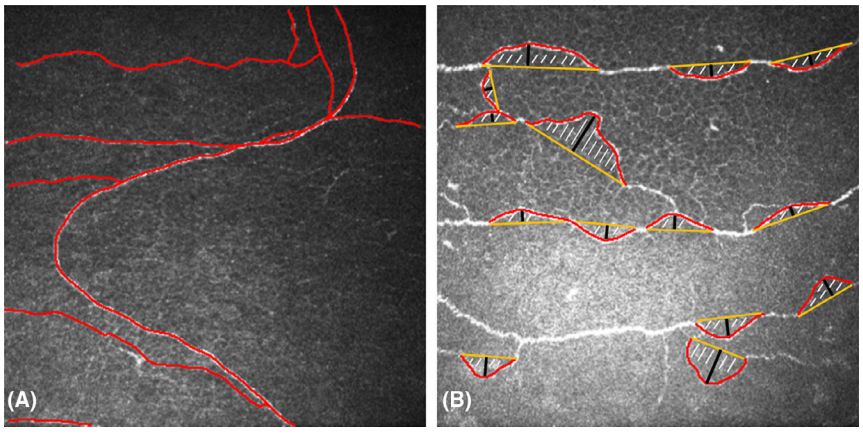

Fig. 1. Corneal confocal microscopy (CCM) images of the subbasal nerve plexus (SNP) (keratoconus, 400 × 400 μm). (A) SNP tracing (red) done by ImageJ® software, long-range tortuosity. (B) SNP tracing (red), area under the curve (hatched), baseline (yellow), amplitude under the curve formed by the SNP (black), short-range tortuosity.

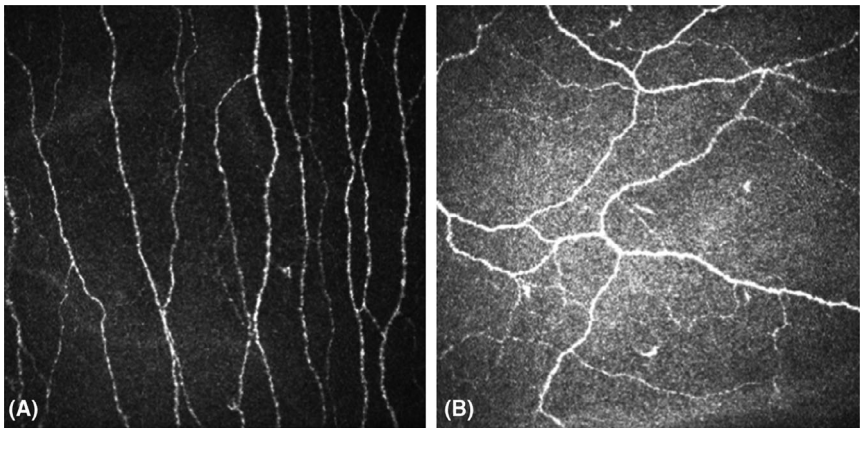

Fig. 2. Corneal confocal microscopy (CCM) images of the subbasal nerve plexus (SNP; 400 × 400 μm). (A) In a healthy cornea, the SNP is of long corneal nerve fibre length (CNFL) and less tortuous. (B) In keratoconus (KC), the SNP is of shorter CNFL with characteristic tortuosity (example here A4B4C4D4 according to Belin's KC classification, Belin & Duncan 2016).

The study adhered to the principles of the Declaration of Helsinki and was approved by the local ethics committee of Saarland (Ethikkommission bei der Ärztekammer des Saarlandes, approval number 96/18).

All subjects were informed about the nature of the study and provided written consent before CCM examination. The diagnosis KC was ensured by clinical slit lamp examination [central or paracentral thinning, hemosiderin deposition (Fleischer Ring), Vogt Striae] and Scheimpflug imaging based on the Belin/Ambrósio Enhanced Ectasia Display and the 'Enhanced Reference Surface' (Oculus Pentacam; Oculus Optikgeräte GmbH, 35582 Wetzlar, Germany) diagnosing KC in case of pathologic anterior or posterior elevation values and a pathologic final *D* value (Duncan, Belin, & Borgstrom 2016). Keratoconus (KC) stages were classified according to Belin's KC stage classification (Belin & Duncan 2016) considering A the anterior radius of curvature, B the back surface radius of curvature, C the corneal pachymetry at thinnest and D the distance best corrected vision. Keratoconus (KC) stages in our patient group reached from A0B2C0D0 to A4B4C4D4 according to this classification, which may also be used to separate progressive from non-progressive KC (Kosekahya et al. 2019). Patient exclusion criteria were neurodegenerative diseases including diabetes, ocular trauma, previous corneal surgery, coexisting corneal pathology and keratitis. Patients wearing contact lenses have not been excluded.

Analysis of the images was performed using the open-source software ImageJ® (version 1.51, Wayne Rasband, National Institutes of Health, Bethesda, MD, USA) and its plugin NeuronJ® (version 1.4.3, Erik Meijering, University of New South Wales, Sydney, Australia, https://imagescience.org/meijering/software/neuronj/). The CNFL was calculated as the length (mm) of nerve fibres per total frame area (400 μm × 400 μm) extrapolated to one square millimetre (Fig. 1A). Statistical analysis was performed using the Mann–Whitney *U*-test and Prism5 software (GraphPad software Inc., San Diego, CA, USA).

The analysis of the SNP revealed an alterated structure in KC corneae. Whilst the SNP in a healthy cornea is of less tortuosity (Fig. 2A), the SNP in KC is curved and tortuous (Fig. 2B).

An attempt to quantify this tortuosity using the open-source software ImageJ® was made by measuring manually (a) the amplitude of the curves formed by the SNP and (b) the area under the curve (AUC) formed by the SNP (Fig. 1B). To measure the amplitudes, an imaginary, ideally straight nerve fibre course was simulated by ImageJ® software and thereafter, the software measured the amplitude (n = 130) of the curve formed by the SNP (Fig. 1B). The AUC (n = 130) of the nerve plexus was measured by manually tracing the curved nerve course and by automatically connecting the beginning and end points of the traced line by ImageJ® software (Fig. 1B). The enclosed area was thereafter calculated by ImageJ® software (Fig. 1B). Small curves with an enclosed area of ≤1.000 μm^2 have been excluded from analysis, as they were present in KC and in healthy corneae. Curves running out of the captured frame were also excluded. In snake-like appearances of the nerves, only the curves within the captured frame were measured.

Results

Keratoconus (KC) is characterized by a progressive and presumed non-inflammatory thinning of the cornea. In the patients' eyes of the study group, the central corneal thickness was significantly lower in KC patients (429.8 ± 81.1 μm) than in healthy corneae (550.3 ± 33.4 μm, $p < 0.0001$, Table 1). Statistical analysis of the CNFL in 390 CCM images of 23 eyes from 23 patients revealed that the CNFL was significantly lower in KC (16.4 ± 1.9 mm/mm^2) compared to healthy corneae (23.8 ± 3.3 mm/mm^2, $p < 0.0001$; mean ± SD; p-value calculated using the Mann–Whitney U-test, Fig. 3A,B). There was no difference in CNFL between contact lens wearing and noncontact lens wearing KC patients ($p = 0.4$). Quantification of the SNP's tortuosity was made by measuring the amplitude and the AUC of the curves formed by the SNP. The amplitudes and the AUCs were significantly larger in KC (values given as median/25th/75th percentile for amplitude 33/23/41 μm and AUC 2839/1545/3444 μm^2) than in healthy corneae (amplitude 24/18/28 μm and area 1870/1193/2327 μm^2, $p < 0.0001$, Fig. 4A,B). Amplitudes and areas under the curve were highly correlated with a Spearman correlation coefficient of $r = 0.803$ ($p < 0.0001$, Fig. 5).

Discussion

Corneal confocal microscopy (CCM) is a non-invasive and valuable tool providing insights into structural changes within the human cornea. This study focuses on the alterations of the SNP in KC based on analysis of the CNFL and a quantification of the tortuous course of the SNP. Whilst the SNP in a healthy cornea has a longer CNFL and is less tortuous, the SNP in KC is of a significantly shorter CNFL with a characteristic tortuosity, which is apparently subject to constant change: The SNP's structure is not static but rather dynamic with the nerve fibres of the SNP centripetally sliding at 5.5–17 μm every day (Patel & McGhee 2008). The apex position and cone size in KC differ inter-individually and therefore also do form obstacles concerning a standardized analysis of the SNP structure (Simo Mannion, Tromans & O'Donnell 2005).

Previous CCM studies estimated a reduced SNP CNFL (Simo Mannion, Tromans & O'Donnell 2005; Niederer et al. 2008; Song et al. 2016; Köhler et al. 2017) by 50% compared to corneae of healthy individuals (Niederer et al. 2008), a rather oblique or horizontal orientation of the nerve fibres (Patel & McGhee 2006) and an abnormal nerve fibre morphology even in early stages of KC (Patel & McGhee 2006). Even in topographically inconspicuous partner eyes of advanced KC patients, the SNP density was lower than in healthy controls (Pahuja et al. 2016), which indicates that subtle changes in the SNP structure precede clinical–morphological manifestations of the disease. Measuring and extrapolating SNP CNFL, however, is not without limitations.

Lagali et al. (2018) found the CNFL to be overestimated by 10% in depth-corrected single images (20 images per eye) and to be underestimated by up to 35% in non-depth-corrected CCM images (20 images per eye). This was attributed to a decreased visualization of the three-dimensional structure of the SNP in non-depth-corrected CCM images. Another study found a CNFL of 19.6 ± 4.2 mm/mm^2 based on the analysis of 4.3 CCM images per eye from 207 eyes of 106 healthy volunteers (age range 15–88 years, Parissi et al. 2013). They reported an underestimation of −20% in density when being based on single images with minimum nerve density and an overestimation of +21% in density when analysing images of maximum nerve density leading to an average CNFL of 23–24 mm/mm^2 in maximum density areas (Parissi et al. 2013). An average CNFL of 22.4 ± 6 mm/mm^2 based on the analysis of three CCM images per eye was found by Niederer et al. (2008). The current study was based on the analysis of 10 raw non-overlapping CCM images per eye and found a CNFL of 23.8 ± 3.3 mm/mm^2 in healthy corneae and 16.4 ± 1.9 mm/mm^2 in KC. These results may therefore be affected on the one hand by overestimation when compared to the results of the aforementioned studies, but they also may be underestimated on the other hand because of the missing depth correction.

Further previous CCM studies pointed out that contact lens wear

Table 1. Summary of patients included and analysed data (based on 10 non-overlapping images per eye from 16 healthy controls and 23 KC patients)

		Healthy controls (n = 16)	Keratoconus (n = 23 patients)	p
Age	± SD	36 ± 19.1	36 ± 10.6	
K-max	± SD	44.9 ± 2.7	63.2 ± 16.3	<0.001
Central corneal thickness	± SD	550.3 ± 33.4	429.8 ± 81.1	<0.0001
SNP CNFL (mm/mm^2)	± SD	23.8 ± 3.3	16.4 ± 1.9	<0.0001
Amplitudes (μm, n = 130)	median/25th/75th Percentile	24/18/28	33/23/41	<0.0001
AUC (μm^2, n = 130)	median/25th/75th Percentile	1870/1193/2327	2839/1545/3444	<0.0001

± SD = mean ± standard deviation, AUC = area under the curve, CNFL = corneal nerve fibre length, SNP = subbasal nerve plexus.

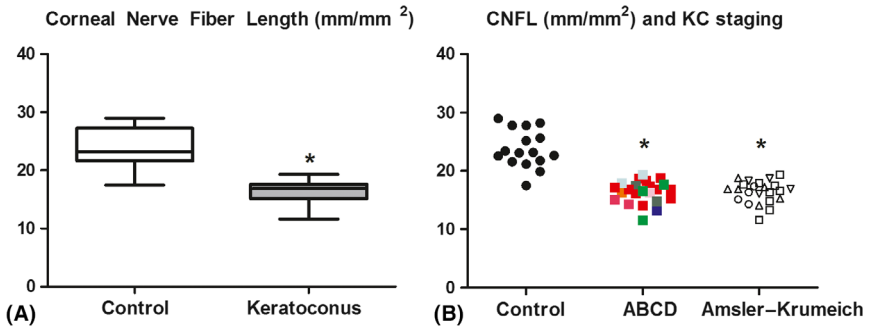

Fig. 3. Subbasal nerve plexus (SNP) corneal nerve fibre length (CNFL) calculated as total length of nerve fibres (mm) per frame area (mm^2). (A) The SNP CNFL in keratoconus (KC) was significantly lower than in control corneae. The p-value (*, <0.0001) was calculated using a Mann–Whitney *U*-test (box with median, 25th and 75th percentile; whiskers representing range of all values). (B) Same data as (A), but individual data including KC staging according to Belin's ABCD classification (Belin & Duncan 2016) in colours and the Amsler–Krumeich (AK) classification in black and white. Red, most advanced stage A4B4; orange, stage A3B4; pink, stage A2B4; purple, stage A2B3; blue, stage A2B2; light blue, stage A1B3; light green, stage A1B2 and dark green, early-stage A0B2. Square, AK stage I; circle, AK stage II; triangle down, AK stage III; triangle up, AK stage IV.

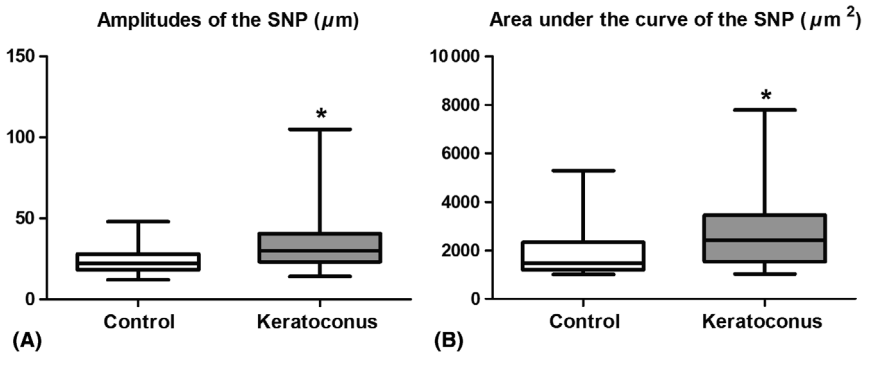

Fig. 4. Analysis of amplitudes and areas under the curve of subbasal nerve plexus (SNPs) in control corneae (16 healthy individuals) and keratoconus (KC; 23 patients) taken from 10 images per individual. The p-value (*, <0.0001) was calculated using a Mann–Whitney *U*-test (box with median, 25th and 75th percentile; whiskers representing range of all values). (A) Amplitudes (μm, $n = 130$) of the SNP (as shown in Fig. 1B, black) were significantly larger in KC compared to control corneae. (B) Areas under the curve (μm^2, $n = 130$, as shown in Fig. 1B, hatched, areas of <1.000 μm^2 excluded) were significantly larger in KC than in control corneae.

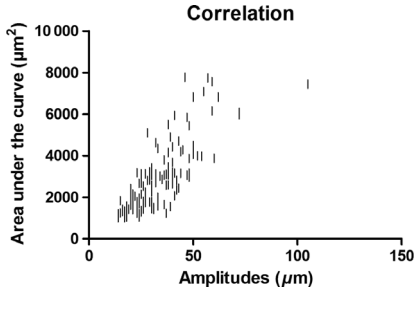

Fig. 5. Correlation of areas under the curve (μm^2) and amplitudes (μm). High correlation with a Spearman correlation coefficient of $r = 0.803$ ($p < 0.0001$).

had no influence on the recorded CNFL in KC (Patel et al. 2002; Oliveira-Soto & Efron 2003; Bitirgen et al. 2013), and therefore, both contact lens wearing and noncontact lens wearing KC patients were included in this study with the result of a comparable CNFL without significant difference ($p = 0.4$) among themselves but with significantly lower CNFL than in the control group ($p < 0.0001$ for both contact lens wearing and noncontact lens wearing KC patients). The significantly lower CNFL in KC might contribute to the reduced corneal susceptibility which has been correlated to the severity of KC (Patel & McGhee 2006).

In the current study, the different CNFL densities could not be assigned to certain stages of KC (according to Belin's ABCD and the Amsler–Krumeich classification, Fig. 3B), which could be because not all stadiums were represented equally, but another study reported a correlation between advanced KC stages and decreasing CNFL (Bitirgen et al. 2015). Because KC is characterized by a progressive ectasia of the cornea, it might be assumed that nerve fibres are pulled towards the peripheral cornea resulting in a rarification of nerve fibres in the central parts of the cornea. Ultrastructural studies of KC by electron microscopy, however, pointed out that the degenerative process leading to nerve fibre rarification is generalized and begins at the corneal epithelium, which degenerates and thus loses its ability to support the nerve fibres by providing nutrients (Teng 1963). Considering the tortuous course of the nerve fibres in KC, many parameters were used to describe and quantify its abnormal structure (Petropoulos et al. 2014; Bitirgen et al. 2015; Pahuja et al. 2016), without, however, measuring the tortuosity itself. This is provided by measuring amplitudes and AUCs as described in this study. Small curves with an enclosed area of ≤1.000 μm^2 were present in KC and in healthy corneae and have, therefore, been excluded from analysis. The main limitations of this method are that (a) these measurements still have to be carried out semi-automatically (tracing manually, calculating automatically) and that (b) many curves, which are running out of the captured frame cannot be included into analysis. Nevertheless, there is a trend towards complete automation: current developments aim to repeatedly display the corneal nerve fibre course using tracking methods in order to carry out progression assessments (Parissi et al. 2013). Two subtypes of tortuosity are reported to exist, the first describing short-range tortuosity with small amplitudes and the second describing long-range tortuosity with large amplitudes of the SNP (Lagali et al. 2015). Based on this finding, the SNP captured on 163 (71%) CCM images in this study would be classified to be of short-range tortuosity, whereas 67 (29%) CCM images revealed a rather long-range tortuosity in KC corneae (Fig. 1).

This study assessed the SNP structure by quantifying the CNFL and the tortuous course of the nerve fibres in

KC and control corneae based on 10 CCM images per eye and per individual (a total of 390 CCM images). Wearing contact lenses or not in the KC group did not influence the results in view of the differences of CNFL in KC patients and healthy controls. Corneal nerve fibre length (CNFL) in KC was about 24% lower than in control corneae. Since mild KC stages were not excluded, it can be assumed that the actual difference is to be set even higher in advanced stages. Measuring the amplitudes and the areas under the curves formed by the SNP enables measuring the SNP's tortuosity itself in KC. Amplitudes and areas under the curve were highly correlated, with the amplitudes' measurement being more suitable in praxi.

Corneal cross-linking is the main stabilizing procedure among the therapeutic options in KC disease. Although the CNFL remains reduced after corneal cross-linking, tortuosity and nerve looping frequency do increase postoperatively (Parissi et al. 2016). Especially early KC are reported to show an increased frequency of nerve loops, crossings and tortuosity (Parissi et al. 2016). The subtle SNP changes as detected by CCM may therefore be helpful in the diagnosis, monitoring and progression assessment of KC when the established topographic diagnostics reach their limits as in topographically inconspicuous partner eyes of advanced KC patients, when doubts about progression do exist or even in advanced KC, when measurement inaccuracies occur.

References

Allgeier S, Winter K, Bretthauer G, Guthoff RF, Peschel S, Reichert KM, Stachs O & Köhler B (2017): A novel approach to analyze the progression of measured corneal sub-basal nerve fiber length in continuously expanding mosaic images. Curr Eye Res **42**: 549–556.

Belin MW & Duncan JK (2016): Keratoconus: the ABCD grading system. Klin Monbl Augenheilkd **6**: 701–707.

Bitirgen G, Ozkagnici A, Malik RA & Oltulu R (2013): Evaluation of contact lens-induced changes in keratoconic corneas using in vivo confocal microscopy. Invest Ophthalmol Vis Sci **8**: 5385–5391.

Bitirgen G, Ozkagnici A, Bozkurt B & Malik RA (2015): In vivo corneal confocal microscopic analysis in patients with keratoconus. Int J Ophthalmol **3**: 534–539.

Duncan JK, Belin MW & Borgstrom M (2016): Assessing progression of keratoconus: novel tomographic determinants. Eye Vis **3**: 6.

Goebels S, Seitz B & Langenbucher A (2013): Diagnostics and stage-oriented therapy of keratoconus: Introduction to the Homburg Keratoconus Center (HKC). Ophthalmologe **9**: 808–809.

Goebels S, Eppig T, Wagenpfeil S, Cayless A, Seitz B & Langenbucher A (2015): Staging of keratoconus indices regarding tomography, topography, and biomechanical measurements. Am J Ophthalmol **4**: 733–738.e3.

Köhler B, Allgeier S, Bartschat A et al. (2017): In vivo imaging of the corneal nerve plexus. Ophthalmologe **7**: 601–607.

Kosekahya P, Caglayan M, Koc M, Kiziltoprak H, Tekin K & Atilgan CU (2019): Longitudinal evaluation of the progression of keratoconus using a novel progression display. Eye Contact Lens **5**: 324–330.

Lagali N, Poletti E, Patel DV et al. (2015): Focused tortuosity definitions based on expert clinical assessment of corneal subbasal nerves. Invest Opthalmol Vis Sci **9**: 5102.

Lagali N, Allgeier S, Guimarães P et al. (2018): Wide-field corneal subbasal nerve plexus mosaics in age-controlled healthy and type 2 diabetes populations. Sci data **5**: 180075.

Müller LJ, Vrensen GF, Pels L, Cardozo BN & Willekens B (1997): Architecture of human corneal nerves. Invest Ophthalmol Vis Sci **5**: 985–994.

Niederer RL, Perumal D, Sherwin T & McGhee CNJ (2008): Laser scanning in vivo confocal microscopy reveals reduced innervation and reduction in cell density in all layers of the keratoconic cornea. Invest Ophthalmol Vis Sci **7**: 2964–2970.

Oliveira-Soto L & Efron N (2003): Morphology of corneal nerves in soft contact lens wear. A comparative study using confocal microscopy. Ophthalmic Physiol Opt **2**: 163–174.

Pahuja NK, Shetty R, Nuijts RM, Agrawal A, Ghosh A, Jayadev C & Nagaraja H (2016): An in vivo confocal microscopic study of corneal nerve morphology in unilateral keratoconus. BioMed Res Int **2016**: 1–5.

Parissi M, Karanis G, Randjelovic S, Germundsson J, Poletti E, Ruggeri A, Utheim TP & Lagali N (2013): Standardized baseline human corneal subbasal nerve density for clinical investigations with laser-scanning in vivo confocal microscopy. Invest Ophthalmol Vis Sci **10**: 7091–7102.

Parissi M, Randjelovic S, Poletti E et al. (2016): Corneal nerve regeneration after collagen cross-linking treatment of keratoconus: a 5-year longitudinal study. JAMA Ophthalmol **1**: 70.

Patel DV & McGhee CNJ (2006): Mapping the corneal sub-basal nerve plexus in keratoconus by in vivo laser scanning confocal microscopy. Invest Ophthalmol Vis Sci **4**: 1348–1351.

Patel DV & McGhee CNJ (2008): In vivo laser scanning confocal microscopy confirms that the human corneal sub-basal nerve plexus is a highly dynamic structure. Invest Ophthalmol Vis Sci **8**: 3409–3412.

Patel SV, McLaren JW, Hodge DO & Bourne WM (2002): Confocal microscopy in vivo in corneas of long-term contact lens wearers. Invest Ophthalmol Vis Sci **4**: 995–1003.

Petropoulos IN, Alam U, Fadavi H et al. (2014): Rapid automated diagnosis of diabetic peripheral neuropathy with in vivo corneal confocal microscopy. Invest Ophthalmol Vis Sci **4**: 2071–2078.

Richter A, Slowik C, Somodi S, Vick HP & Guthoff RF (1997): In vivo imaging of corneal innervation in the human using confocal microscopy. Ophthalmologe **2**: 141–146.

Simo Mannion L, Tromans C & O'Donnell C (2005): An evaluation of corneal nerve morphology and function in moderate keratoconus. Cont Lens Anterior Eye **4**: 185–192.

Song P, Wang S, Zhang P, Sui W, Zhang Y, Liu T & Gao H (2016): The superficial stromal scar formation mechanism in keratoconus: a study using laser scanning in vivo confocal microscopy. BioMed Res Int **2016**: 7092938.

Teng CC (1963): Electron microscope study of the pathology of keratoconus. Am J Ophthalmol **55**: 18–47.

Received on November 3rd, 2019.
Accepted on March 16th, 2020.

Correspondence:
Elias Flockerzi MD
Department of Ophthalmology
Saarland University Medical Center
66421 Homburg
Germany
Tel: +49-6841-16-22302
Fax: +49-6841-16-22479
Email: elias.flockerzi@uks.eu

Loay Daas and Berthold Seitz declare that they do not have any financial disclosures. Elias Flockerzi has received a travel grant to the Second and Third Ophthalmology Cystinosis Forum (Orphan Europe, Ulm, Germany) and an invitation to a seminar on presentation training organized by the Santen GmbH (Munich, Germany). All authors contributed to this work by providing data, revising the manuscript, approving it for publication and agreeing to take full responsibility for all aspects of this work.